Automatic Gait-Pattern Adaptation Algorithms for Rehabilitation With a 4-DOF Robotic Orthosis

Sašo Jezernik, Gery Colombo, and Manfred Morari

***Abstract*—This paper presents newly developed algorithms for automatic adaptation of motion for a robotic rehabilitation device. The algorithms adapt the gait pattern of patients that walk on a treadmill. Three different algorithms were developed. The first one is based on inverse dynamics and online minimization of the human–machine interaction torque. The second one is based on direct dynamics and estimation of the desired variation in the gait-pattern acceleration. The third algorithm is based on impedance control and direct adaptation of the gait pattern angular trajectories. The algorithms were tested and compared in computer simulations and actual experiments on healthy subjects and patients. In simulations, all algorithms have adapted the gait pattern toward the desired one, which led to a greater than 40% reduction of interaction torques. The impedance-control-based algorithm performed best in the experiments.**

***Index Terms*—Adaptive control, rehabilitation of locomotion, reference joint-angle trajectory adaptation, treadmill training.**

I. Introduction

Rehabilitation of locomotion in stroke and spinal cord injured (SCI) individuals has seen major developments during the last two decades (Barbeau *et al.* [1]). One important new rehabilitation technique is so-called *treadmill training* (Hesse *et al.* [5], Wernig *et al.* [13], Dietz *et al.* [3]). In manual treadmill training, the patient is standing on a treadmill and his body weight is reduced by a special suspension system. The walking-like leg movements are generated and/or assisted by manual handwork of two physiotherapists. To increase the duration of the training and to reduce the effort of the physiotherapists, the treadmill training has been automated. A four-degrees-of-freedom (DOF) robotic orthosis called *Lokomat* was built for this purpose (Colombo *et al.* [2]).

The Lokomat is an orthosis with actuated hip and knee joints (Fig. 1). It is adjustable in the length of the upper and lower leg segments, and the patient's hip width and leg circumference. The actuation is done by DC motors, and the angles are measured by potentiometers. The reference trajectories that are used to control the motion are physiological hip and knee angle trajectories. The Lokomat structure is fixed to the treadmill by a four-bar linkage in order to provide lateral plane stabilization. The patient's legs are connected to the Lokomat by three braces per leg.

The regular patient training with the Lokomat is performed with a fixed gait pattern that is realized by position control of the joint angle trajectories. On the other hand, it is important to insure that the patient himself is actively walking, and not only that his legs are passively moved by the Lokomat. This idea led to the development of automatic gait-pattern adaptation algorithms reported in this paper. These algorithms enable patients that have *some degree of voluntary locomotor capability* to walk in the Lokomat actively with a variable gait pattern. Training with an adaptive gait pattern has the following advantages over the training with a fixed gait pattern: 1) active movements and muscle contractions versus passive movements/passive muscles; 2) more physiological and variable sensory input to the central nervous system (CNS) centers; and 3) increased motivation of the patient, who can now control the movement of the Lokomat. Especially, 1) and 2) might lead to better rehabilitation of the CNS.

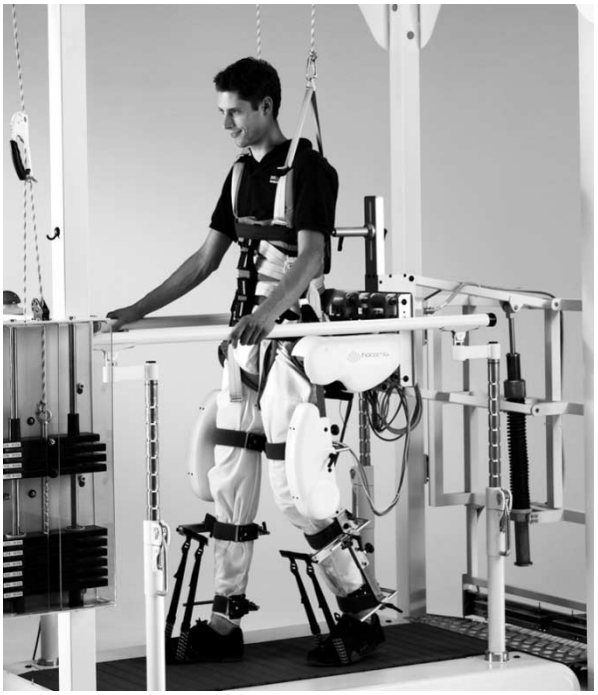

Fig. 1. A healthy subject suspended over the treadmill and walking with the use of the robotic orthosis Lokomat.

The focus of the paper will be on the development and realization of the algorithms for automatic gait-pattern adaptation. The first algorithm produces gait-pattern adaptation by first estimating the human–robot interaction torques and then by adapting the angle trajectories in a way that leads to reduction in the interaction torques. The second algorithm estimates the human–robot interaction torques and then translates this into the desired change in the trajectory accelerations. In the third algorithm, the impedance control generates a prespecified open-loop relationship between the interaction torques and the allowed position deviations. This approach allows direct adaptation of the trajectories from the measured position deviation or from the estimated interaction torques.

The gait-pattern adaptation itself was achieved by generating a suitable variation in the reference hip and knee angle trajectories. The performance of the algorithms was tested in computer simulations and in experiments with healthy subjects and five SCI patients. Preliminary results were reported in Jezernik *et al.* [7] and Jezernik *et al.* [8], [9].

II. Methods

A. Force-Sensing System

In order to sense the intention of the patient to change the gait pattern (based on his active effort and physical interaction exerted onto the Lokomat), a suitable sensory input to the gait-pattern adaptation algorithm is needed. Obvious signals that can be used for this purpose are the interaction forces between the Lokomat and the patient. These

Manuscript received February 9, 2003; revised August 3, 2003. This paper was recommended for publication by Associate Editor P. Dario and Editor R. Taylor upon evaluation of the reviewers' comments. This work was supported by The Swiss Commission for Technology and Innovation under Project 4005.1.

S. Jezernik and M. Morari are with the Swiss Federal Institute of Technology (ETHZ), Automatic Control Laboratory, 8092 Zürich, Switzerland (e-mail: jezernik@control.ee.ethz.ch). S. Jezernik is also with the Spinal Cord Injury Center ParaCare, University Hospital Balgrist, 8008 Zürich, Switzerland.

G. Colombo is with the Spinal Cord Injury Center ParaCare, University Hospital Balgrist, 8008 Zürich, Switzerland.

Digital Object Identifier 10.1109/TRA.2004.825515

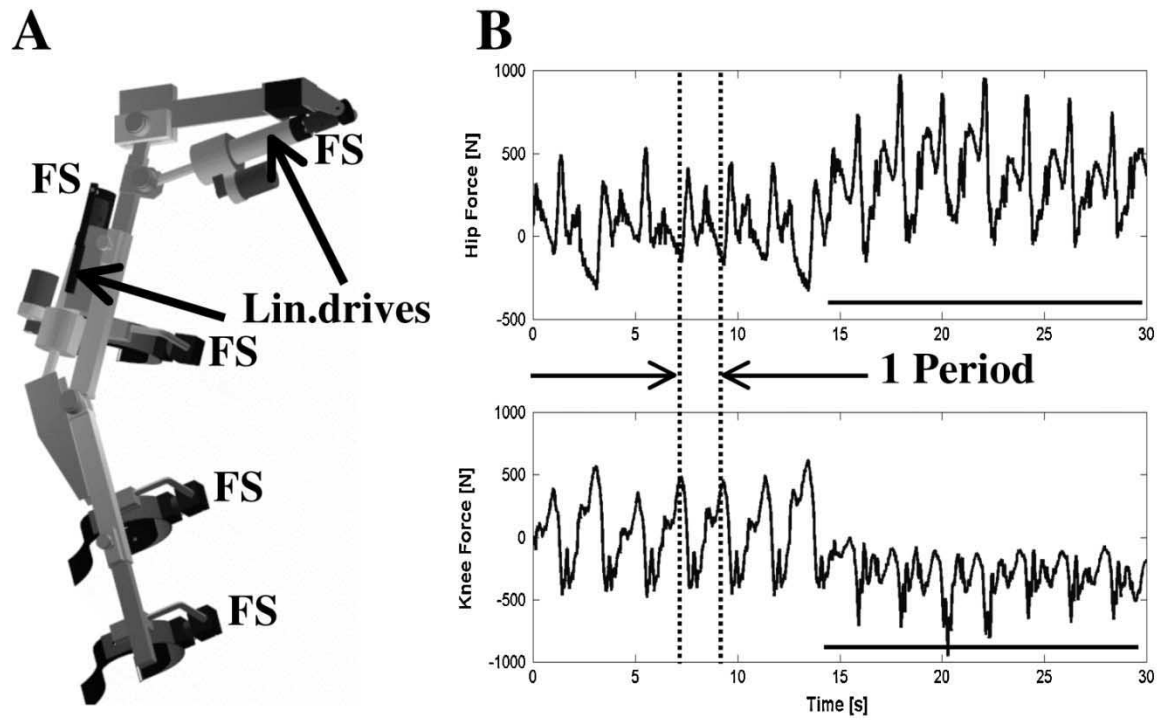

Fig. 2. (a) Drawing of one Lokomat's leg together with the linear drives and the force measurement systems. The hip and knee joints are actuated by two linear drives containing two DC motors. The first measurement system consists of two FSs located in series with the linear drives. The second measurement system consists of three FSs placed in series with the leg braces. The first system was used in the subsequent experiments. (b) Demonstration that the hip (top) and knee (bottom) forces change when the subject tries to change the nominal gait pattern (during the time indicated by bars).

forces are generated by the patient, and act on the Lokomat system in a dynamic way. Two force-sensing systems have been developed to measure these forces [Fig. 2(a)]: 1) a system using two 1-axial force sensors (FS) placed in series to the linear drives that move the Lokomat segments; and 2) a system using three 3-axial FSs placed in series to the patient–Lokomat leg contact surfaces (leg braces). Both systems were evaluated via comparison of the hip and knee torques calculated from the force measurements. The evaluation confirmed that the active patient effort was contained in these measurements [Fig. 2(b)], and furthermore, that the two systems were equivalent. Because of this result, the simpler and cheaper system 1) was used in all subsequent experiments. Force sensing not only allowed for measurement of the human–Lokomat interaction, but also enabled implementation of force and impedance control schemes.

B. Mathematical Model

Each leg of the Lokomat was modeled as a double pendulum with distributed masses using the standard robotic dynamic equation derived by the Lagrange Principle

$$M_{\mathrm{ORT}}(q)\ddot{q} + C_{\mathrm{ORT}}(q,\dot{q}) + G_{\mathrm{ORT}}(q) = \tau_{\mathrm{BS}} + \tau_{\mathrm{PAT}} - \tau_{\mathrm{TM}} - \tau_{\mathrm{FRICT,JOINTS}} \quad (1a)$$

$$\tau_{\mathrm{BS}} = K_T(q)\tau_{\mathrm{DC}}(i_{\mathrm{DC}}) - \tau_{\mathrm{FRICT,BS+DC.}} \quad (1b)$$

In these two equations, $q \in \Re^2$ is the generalized position vector comprising the hip and knee angles, $M \in \Re^{2\times 2}$ is a symmetric, positive definite inertia matrix, $C \in \Re^2$ is a term representing the Coriolis and centrifugal torques, and $G \in \Re^2$ is a term representing the gravity torques. The $\tau \in \Re^2$ terms on the right-hand side of (1a) are the torques acting onto the orthosis. τ_{BS} is the ball-screw torque of linear drives acting onto the links of the orthosis generated by DC motors, τ_{PAT} is the torque originating from the patient–orthosis interaction, τ_{TM} is the torque originating from the patient–treadmill interaction, and $\tau_{\mathrm{FRICT,JOINTS}}$ is the joint friction torque. K_T is the torque transmission gain (range for hip $=$ 297–325; for knee $=$ 194–246) that has a nonlinear geometrical dependency. In (1b), the $\tau_{\mathrm{FRICT,BS+DC}}$ is the friction torque term comprising the ball-screw and DC motor friction. τ_{DC} is the DC motor torque ($\tau_{\mathrm{DC}} = k_m^* i_{\mathrm{DC}}$), and is (except in the impedance control scheme, see below) generated by a proportional derivative (PD) position control law

$$\tau_{\mathrm{DC}} = k_m \cdot i_{\mathrm{DC}} = k_m \cdot K_P(q_r - q) + k_m \cdot K_D(\dot{q}_r - \dot{q}). \quad (2)$$

The position controller needs to generate the torque necessary for the reference motion of the orthosis, τ_{ORT}

$$\tau_{\mathrm{ORT}}(q_r) = M_{\mathrm{ORT}}(q_r)\ddot{q}_r + C_{\mathrm{ORT}}(q_r,\dot{q}_r) + G_{\mathrm{ORT}}(q_r) \quad (3)$$

and needs to compensate the other torque terms τ_{PAT} and τ_{TM} as well as the friction terms.

The modeled terms include $M, C,$ and G. The τ terms in (1a) were not modeled. Sensor measurements yielded q (goniometers) and τ_{BS} FSs.

Equations (1) can be rewritten as

$$\tau_{\mathrm{BS}} = K_T(q)\tau_{\mathrm{DC}}(i_{\mathrm{DC}}) - \tau_{\mathrm{FRICT,BS+DC}} = \tau_{\mathrm{ORT}} + \tau_{\mathrm{PAT,PAS}} - \tau_{\mathrm{PAT,ACT}} + \tau_{\mathrm{TM}} + \tau_{\mathrm{FRICT,JOINTS}} \quad (4)$$

where the patient torque τ_{PAT} was split into an active and passive component ($\tau_{\mathrm{PAT}} = \tau_{\mathrm{PAT,ACT}} - \tau_{\mathrm{PAT,PAS}}$). The passive patient torque is the torque that needs to be compensated for by the position controller to move the legs of the passive patient. If, on the other hand, the patient will influence the gait voluntarily, he will produce an additional, active torque component $\tau_{\mathrm{PAT,ACT}}$.

For the sake of simplicity and convenience, we have further combined the terms $\tau_{\mathrm{PAT,PAS}}$ and τ_{ORT} to a term $\tau_{\mathrm{PAT,PAS+ORT}}$, which was again modeled in the same way as the term τ_{ORT} [(3)], but with adapted terms $M_{\mathrm{PAT+ORT}}$, $C_{\mathrm{PAT+ORT}}$, and $G_{\mathrm{PAT+ORT}}$. These were recalculated with assumed additional leg masses ($m_i = m_{i,\mathrm{LOK}} +$

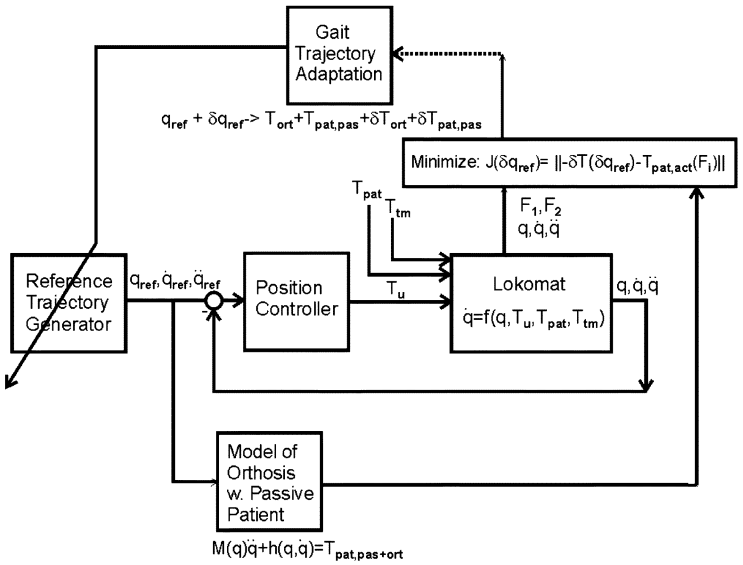

Fig. 3. Block diagram of the inverse-dynamics-based gait-pattern adaptation algorithm. The Lokomat is controlled by a position controller with reference hip and knee joint angle trajectories. The force measurement (yielding F_1 and F_2) is used together with a model of the orthosis and a passive patient to adapt the reference trajectories (q_r) according to the optimization of the functional J.

$m_{i,\mathrm{PAT}}$), whereby the thigh mass was estimated as 10.6%, and the shank mass as 6.4% of the total body weight, respectively.

C. Adaptation of the Gait Pattern

The reference trajectories were parameterized with parameters a_1, c_1, d_1 (hip trajectory parameters), and parameters a_2, c_2, and d_2 (knee trajectory parameters) in the following way (with $\varphi_{i,\mathrm{gen}}$ being the nominal physiological trajectory):

$$\varphi_i = a_i \cdot \varphi_{i,\mathrm{gen}}\left(\frac{t}{c_i}\right) + d_i, \quad i = 1, 2. \tag{5}$$

The parameter a scales the amplitude, parameter c stretches the time and influences the period of the leg motion, and parameter d (offset) changes the amount of the hip/knee flexion and extension. By varying the set of parameters $a - d$, different hip and knee joint angle trajectories, and therefore, different gait patterns are produced. The parameters c_1 and c_2 are, however, not independent (due to the fact that the hip and knee trajectories need to have the same period). They were after initial calculation substituted by their weighted sum, i.e., $c_{i,\mathrm{ACTUAL}} = w_1 * c_{1,\mathrm{CALC}} + w_2 * c_{2,\mathrm{CALC}}$ for $i = \{1, 2\}$. The weights were typically set to 0.5. The additional DOF for parameter c was chosen as the change of period could depend more on the interaction information obtained from the hip or knee measurements.

The above parameterization was chosen as it was shown that the class of adapted trajectories $\{\varphi_i\}$ could describe sufficiently well the trajectories that were measured while subjects were walking in the unpowered Lokomat with different gait patterns.

D. Inverse-Dynamics-Based Joint-Angle Adaptation Algorithm

This algorithm evolved from the analysis of the Lokomat–patient interaction. Our hypothesis was that, in the case of completely synchronized movement of the Lokomat and the patient, there should be minimal interaction between these two coupled systems that will, however, increase in case of desynchronization. Ideally, the interaction forces (torques) should be zero if the patient exactly follows the motion of the Lokomat, and they should be unequal to zero if he/she tries to move in a different way than the Lokomat. The developed indirect joint-angle adaptation algorithm is based on the inverse dynamics representation of the problem and works via minimization of the interaction torques.

In a first step, the overall torques are measured using the force measurement system, and the interaction torques estimated from the overall torques. Specifically, we estimate the active patient torque component $\tau_{\mathrm{PAT,ACT}}$ [see (4) above] by calculating a moving average of the torque measurement over the last N strides and subtracting from it the moving average estimate of the total torque during the past steps $2N - 1$ until N. The moving averages were calculated in a recursive way with exponential forgetting. With this approach, the active patient torque estimate contains the changes in the overall measured torque between the time interval $[-N+1, 0]$ and the time interval $[-2N+1, -N]$. This calculation was compared to a calculation where the initially averaged baseline torque (with passive patient) was afterwards subtracted from the overall torque measurement, and also to a calculation where the baseline torque was modeled according to modified (3) ($\tau\mathrm{PAT}, \mathrm{PAS} + \mathrm{ORT}$ terms). In all three approaches, the results were qualitatively the same, but the moving average approach performed most robustly. This was the case, since the "double" moving average estimation with exponential forgetting was able to zero different bias torque terms that arose after the patient has changed the gait pattern.

After obtaining the estimate of the active patient torque, a variation in the reference trajectories q is calculated in such a way that the torque variation resulting from this reference trajectory variation will cause a reduction in the active patient torque that was produced by the patient. The necessary calculations are performed online by means of nonlinear optimization of the following functional:

$$J(\delta q_r, F_1, F_2) = \sum_k \|-\tau_{\mathrm{PAT,ACT}}(F_1, F_2)_{(k)} - \delta\tau(\delta q_r)_{(k)}\|_2^2$$
$$\delta q_{r-\mathrm{adapt}} = \arg\min_{\delta q_r} J(\delta q_r, F_1, F_2) \tag{6}$$

where F_1 and F_2 are the measured ball-screw forces needed for the online estimation of $\tau_{\mathrm{PAT,ACT}}$. This algorithm is termed *indirect joint-angle adaptation*, as the adaptation of the angle trajectories is performed via minimization of a torque functional (and not directly via kinematics). The corresponding block diagram is shown in Fig. 3.

Equation (6) means that the variation in the torque $\delta\tau$ produced by variation in the reference trajectories will lead to a diminished active-patient torque component $\tau_{\mathrm{PAT,ACT}}$.

$\delta\tau$ is calculated from the mathematical model according to the following equation:

$$\begin{aligned}\delta\tau(\delta q_r) = {} & M_{\mathrm{PAT+ORT}}(q_r+\delta q_r)(\ddot{q}_r+\ddot{\delta}q_r)\\ & + C_{\mathrm{PAT+ORT}}(q_r+\delta q_r, \dot{q}_r+\dot{\delta}q_r)\\ & + G_{\mathrm{PAT+ORT}}(q_r+\delta q_r)\\ & - M_{\mathrm{PAT+ORT}}(q_r)\ddot{q}_r - C_{\mathrm{PAT+ORT}}(q_r,\dot{q}_r)\\ & - G_{\mathrm{PAT+ORT}}(q_r). \end{aligned} \tag{7}$$

The minimization of the cost functional J is performed over the parameter space spanned by $a_1 - d_2$.

Since the gait-pattern adaptation needs to be performed in real time, a simple and fast minimization algorithm had to be used. We chose the steepest descent algorithm to calculate the parameters that minimize J. The parameters p were updated in the following way:

$$p_{n+1} = p_n - \eta_{p,n}\frac{\partial J}{\partial p}|_{p_n} \quad p \in \{a_1, c_1, d_1, a_2, c_2, d_2\} \tag{8}$$

where η_p stands for the step size, and n is the iteration number. The step size was taken to be a decreasing geometric sequence

$$\eta_{p,n+1} = q \cdot \eta_{p,n}, \quad q < 1. \tag{9}$$

In the minimization, $n = K$ iterations of the gradient search are performed after selecting the initial parameter values ($a_{i0} = 1, c_{i0} = 1, d_{i0} = 0$), and the initial step sizes $\eta_{p,0}$. To quantify the quality of the minimization of J after K iterations (separately for the hip and the knee torques), the normalized factors Z_1 (hip) and Z_2 (knee) were calculated

$$Z_i = \frac{\|-\tau_{\mathrm{PAT,ACT}_i} - \delta\tau_i\|}{\sqrt{\|\tau_{\mathrm{PAT,ACT}_i}\|^2 + \|\delta\tau_i\|^2}}. \tag{10}$$

Z equals 0 in the case of ideal minimization, where the variation $\delta\tau$ exactly cancels the active-patient torque variation $\tau_{\mathrm{PAT,ACT}}$, and is upper bounded by the square root of two.

E. Direct-Dynamics-Based Joint-Angle Adaptation Algorithm

To reduce the model dependency of the gait-pattern adaptation algorithm described in Section II-D, another variant of the algorithm was developed, which is based on the direct dynamics formulation of the problem.

The direct dynamics equation reads

$$\ddot{q} = M^{-1}\{\tau_{\mathrm{BS}} - \tau_{\mathrm{TM}} - \tau_F - C - G\} + M^{-1}\tau_{\mathrm{PAT,ACT}}. \tag{11}$$

By examining this equation, we can see and further assume that the last term actually represents a variation in the acceleration of the joint-angle trajectories that the patient would like to achieve. This assumption forms the basis of the direct-dynamics-based joint-angle adaptation algorithm. The idea is to estimate again the term $\tau_{\mathrm{PAT,ACT}}$ via FS measurements (the same estimation technique as described above was used) in order to calculate the variation in acceleration, and to form adapted acceleration by adding the scaled variation to the old acceleration

$$\ddot{\delta}q = -M(q)^{-1}\delta\tau_{\mathrm{PAT,ACT}} \Rightarrow \ddot{q}_{\mathrm{NEW}} = \ddot{q}_{\mathrm{OLD}} + w\cdot\ddot{\delta}q. \tag{12}$$

w is the scaling vector that affects the extent of adaptation.

The adaptation of the parameters a and c is now performed in a straight way via minimization of the following functional:

$$J(\delta q_r, F_1, F_2) = \sum_k \|\ddot{q}_{\mathrm{NEW}}(k) - \ddot{q}_{\mathrm{OLD}}(k)\|_2^2. \tag{13}$$

However, the acceleration vector does not contain any information about parameters d, due to double differentiation of (5) The parameters d are, therefore, still adapted by minimization of the torque functional (6) as in the indirect joint-angle adaptation.

The combined minimization was performed by steepest descent as described in Section II-D. To quantify the quality of the minimization of the torque functional J (13) over d_1 and d_2, factors Z_1 (hip) and Z_2 (knee) were calculated as in the indirect adaptation approach (10).

Furthermore, we have also calculated the extent of minimization of (13) by calculating the following two factors Z_3 and Z_4 ($i = 3$ for the hip and $i = 4$ for the knee trajectory):

$$Z_i = \frac{\|\ddot{q}_{i,\mathrm{NEW}} - \ddot{q}_{i,\mathrm{OLD}}\|}{\sqrt{\|q_{i,\mathrm{NEW}}\|^2 + \|\ddot{q}_{i,\mathrm{OLD}}\|^2}}, \quad i = 3, 4. \tag{14}$$

An important advantage of the direct versus inverse dynamics approach is that the former is less dependent on modeling. For the adaptation of the parameters a and c, only the knowledge of the inertia matrix M is actually needed, as opposed to requirements of the knowledge of the terms $M, C,$ and G in the indirect approach. The direct-dynamics-based algorithm can be represented with a similar block diagram, as shown in Fig. 3.

Here we would also like to point out a similarity in the two developed adaptation approaches. Rewriting (7) and denoting the terms $X(q+\delta q) - X(q)$ by ΔX yields

$$\begin{aligned}\delta\tau(\delta q) = {} & \Delta M_{\mathrm{PAT+ORT}}\ddot{q} + M_{\mathrm{PAT+ORT}}(q+\delta q)\ddot{\delta}q\\ & + \Delta C_{\mathrm{PAT+ORT}} + \Delta G_{\mathrm{PAT+ORT}}\end{aligned} \tag{15}$$

which gives the following expression for the variation in the acceleration achieved by the indirect joint-angle adaptation algorithm to be compared with (12):

$$\ddot{\delta}q = M(q+\delta q)^{-1}[-\Delta M\ddot{q} - \Delta C - \Delta G] + M(q+\delta q)^{-1}\delta\tau. \tag{16}$$

For small $\Delta M, \Delta C$, and $\Delta G (\Delta X \to 0)$, this equation gets the same form as (12) since the minimization of (6) yields $\delta\tau \approx -\tau_{\mathrm{PAT,ACT}}$. However, the ΔX terms will not necessarily be small.

F. Impedance-Control-Based Joint-Angle Adaptation Algorithm

The development of the algorithms described in Sections II-D and E was paralleled by the development of an alternative, impedance-control-based algorithm. The impedance control is traditionally used in problems involving robot-environment interaction (contact problem), because of the possibility of combined *contact-free position* and *contact-force control* (Hogan [6]). In the case of Lokomat training, we actually also deal with the patient–Lokomat interaction. This is the reason that led us to develop an impedance control scheme for the Lokomat. Impedance control aims at controlling the relationship between the manipulator force and the deviation between the desired and actual manipulator position. This relationship is specified in an open-loop way, and equals the physical impedance Z. Impedance can be of zero order (stiffness), or of higher order (usually first or second order). The impedance control is conventionally realized by a nonlinear control law derived by Hogan [6], or by an inner-position control loop and an outer-position compensating loop based on force sensing (see, for example, Šurdilović and Čojbašić [12] or Siciliano and Villani [11]). The nonlinear control law is often associated with stability problems. Suitability of both control schemes for controlling the Lokomat is currently under investigation at our center. The impedance control scheme that was realized and is reported here has a different structure, depicted in Fig. 4. The impedance controller consists of an inner proportional integral (PI) force-control loop and an outer PD position-control loop. Since the Lokomat position sensors directly measure the joint angles and the Lokomat FSs the forces generated by the linear drives, the impedance relationship equals

$$F \approx F_{\mathrm{REF}} = [K_P + K_D s]\cdot(q_{\mathrm{REF}} - q) \tag{17}$$

where the PD controller generates the reference force F_{REF}, and where the actual measured force is denoted by F. Higher impedance $|Z(s)| = |K_P + K_D s|$ therefore results in smaller position deviations, and vice

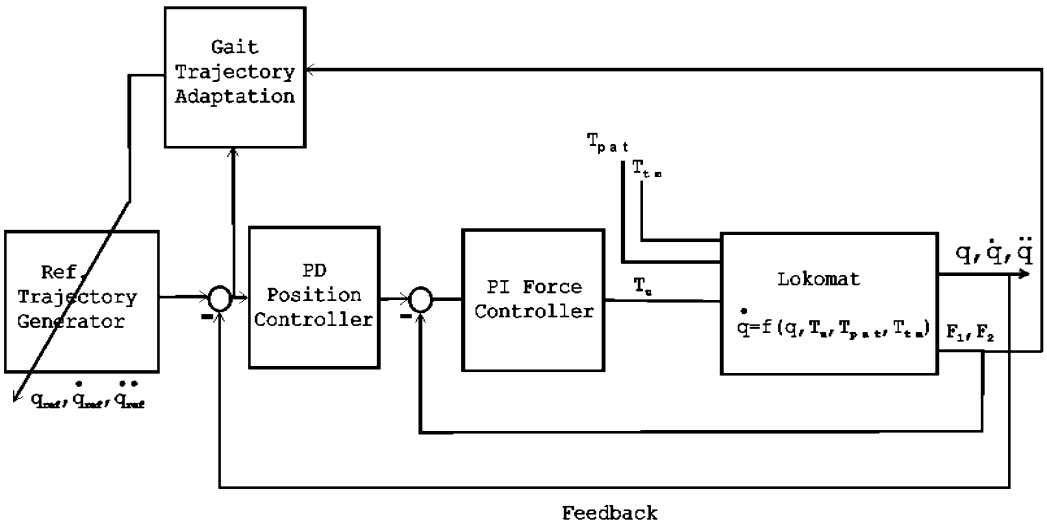

Fig. 4. Block diagram of the impedance-control-based gait-pattern adaptation algorithm. The Lokomat is controlled by a cascaded position and force controllers that realize impedance control. The measured or estimated (via force measurement) position deviations are then used to directly adapt the reference joint angle trajectories according to the patient's effort.

versa. Because of the linearity of the impedance relation, additional external forces cause additional position deviations.

The human-Lokomat interaction will lead to the additional, active patient torque that will be exerted onto the Lokomat. This interaction will cause a change in the measured forces and a change in the position deviations. The position deviations can be obtained directly from the position measurement, or estimated from the change in the measured force and by considering the predefined impedance relation. The latter approach was selected because of the better quality of the force measurement signal, compared with the position measurement. The formula that estimates the desired change in the position trajectories then reads

$$\Delta e = \frac{1}{[K_P + K_D s]} \cdot \Delta F \tag{18}$$

where the ΔF is calculated from the estimated $\tau_{\mathrm{PAT,ACT}}$ (estimated by subtraction of two moving averages of the overall torque measurement, as explained in Section II-D). The adaptation law for the reference trajectories equals

$$q_{\mathrm{REF,NEW}} = q_{\mathrm{REF,OLD}} - w \cdot \Delta e \tag{19}$$

where w serves as a scaling factor to change the extent of adaptation. The actual adaptation of the reference trajectories is carried out by minimization of the following functional over the parameter space spanned by p_i:

$$J(p_i) = \sum_k \| q_{\mathrm{REF,NEW}_{(k)}} - q_{\mathrm{REF}}(p_i)_{(k)} \|_2^2 \tag{20}$$

where the parameterized trajectories and the minimization of J (20) is performed in the same way as described in Sections II-D and E. The extent of minimization is again verified by calculating the Z factors analogously to (14).

G. Evaluation of the Algorithms in Computer Simulations

The computer simulation models were developed in MATLAB/Simulink (MathWorks, USA) and the gait-pattern adaptation algorithms were coded in C as Simulink S-Functions. To test and compare the developed algorithms, a human–Lokomat interaction model was used. This model calculated the interaction torques (active-patient torques) by comparing the prespecified desired Lokomat motion with the actual Lokomat motion, and by assuming that the interaction torques resulted from a virtual spring-like coupling between the desired and the actual position of the Lokomat braces. The spring stiffnesses were set to values that yielded realistic magnitudes of the active-patient torques.

To test the inverse and direct-dynamics-based algorithms, it was enough to input the interaction torques into the adaptation algorithms (MATLAB S-functions) that have then calculated the resulting hip and knee adaptation parameters $a - d$. This allowed for direct comparison of these two algorithms. However, to test the impedance-control-based adaptation algorithm, it was necessary also to simulate the Lokomat and the closed-loop impedance controller. A quantitative comparison of the simulation results of the latter algorithm with the former ones was thus not meaningful.

The simulations were used to determine the extent of adaptation (by comparison of the desired, initial, and adapted motion), the corresponding interaction torque reduction, and the achieved minimization of the corresponding functionals (by the use of the Z factors). The Wilcoxon signed rank test was used to compare the indirect and direct-dynamics-based algorithms.

H. Real-Time Realization

The Real-Time-Workshop and xPC packages were used to translate and compile the MATLAB/Simulink model into a real-time executable program. The real-time program executed at a sampling time of 1 ms. The output of the gait-pattern adaptation algorithms changed every 2 s (frequency of trajectory parameter adaptation). The xPC package allowed for online sampling and offline representation of the Simulink signals of interest. We have also developed a special LabView graphical user interface (GUI) that allowed us to change model parameters and to sample and display different signals of interest.

I. Experimental Evaluation

The gait-pattern adaptation algorithms have been tested in several experiments with healthy subjects, as well as with five SCI patients (lesion levels: C4, C7, T9, and 2x L2; age: 38–62 years). The experimental evaluation included: a) an initial blinded study with enabled and disabled adaptation; b) experiments where the subjects started to walk with a nominal gait pattern and were then asked to change this gait pattern to another gait pattern; and c) experiments where the subjects started walking with a rather unphysiological gait pattern and then tried

TABLE I
REDUCTIONS IN RELATIVE ERRORS (COLUMNS ONE AND TWO) AND REDUCTIONS IN INTERACTION TORQUES (COLUMNS THREE AND FOUR) ACHIEVED BY THE ADAPTATION ALGORITHMS IN COMPUTER SIMULATIONS. ERROR REDUCTIONS WERE CALCULATED AS REDUCTIONS BETWEEN THE DIFFERENCE DESIRED VERSUS INITIAL (UNADAPTED), AND DESIRED VERSUS ADAPTED JOINT-ANGLE TRAJECTORIES. VALUES REPRESENT MEANS ± STANDARD DEVIATIONS (ADAPTATION TO $10/7$ DIFFERENT DESIRED TRAJECTORIES WAS TESTED FOR THE FIRST TWO/THE THIRD ALGORITHM, RESPECTIVELY)

algorithm	relative error change in hip trajectory	relative error change in knee trajectory	relative change in the hip interaction torque	relative change in the knee interaction torque
Indirect dynamics based	-41.1±24.9 %	-11.5±15.0 %	-55.9±14.7 %	-47.6±17.6 %
Direct dynamics based	-61.2±14.8 %	-25.2±20.0 %	-55.6±5.5 %	-52.8±5.0 %
Impedance control based	-42.5±16.0 %	-20.4±16.5 %	-48.7±5.2 %	-48.5±8.8 %

to adapt it to their nominal, preferred gait pattern. Experiments under a) and b) included trials where the subjects tried to modify the gait pattern to walk with larger/smaller steps, increased/decreased hip/knee flexion, or a different speed. Experiments a), b), and c) were done with healthy subjects, while the patients have participated in experiments b) and c).

All experiments were done at a fixed treadmill speed of either 1.8 or 1.9 km/h (approximate stride period 2 s) and with 50% body weight unloading for the healthy, and 50%–90% unloading for the SCI patients. The duration of a trial was usually 120 or 200 s (60–100 strides). At the beginning of each trial, the subjects were asked to follow the reference motion of the Lokomat. After the initial 30 strides (usually after 80 s), they were asked to try to modify the gait pattern.

Analysis of the experimental data was performed analogously to the computer simulation analysis. Additionally, after each trial, we asked the subjects if they felt the adaptation, and if they felt any difference between the initial and the final gait pattern.

III. RESULTS

A. Simulation Results

All three algorithms achieved substantial adaptation that led to reduction in the interaction torques that was typically greater than 40%. The adaptation of the hip trajectory was always toward the desired trajectory (for all three algorithms). In most cases, the adapted knee trajectory moved closer to the desired trajectory, but in some cases, the adaptation led to increased deviation from the desired knee trajectory. This depended on the choice of the desired motion parameters $a_{1,\mathrm{des}} - d_{1,\mathrm{des}}$ and $a_{2,\mathrm{des}} - d_{2,\mathrm{des}}$. It turned out that better overall knee adaptation was achieved by the direct-dynamics-based algorithm than the indirect-dynamics-based one (see the upper part of Table I). However, the Wilcoxon signed rank test revealed that neither of the reduction differences between the two algorithms was statistically significant ($p > 0.14$ at $\alpha = 0.05$). The simulation results for the impedance-control-based algorithm are listed in the bottom part of Table I.

Because of the coupling of the interaction torques, the knee interaction torque was always reduced, even in cases where the actual knee trajectory adaptation deviated more from the desired knee trajectory than the initial one.

Fig. 5 shows the interaction torques (panel A) and Z factors (panels B and C) for the direct-dynamics-based algorithm and adaptation to the desired motion specified by $a_{1,\mathrm{des}} = 1.05, c_{1,\mathrm{des}} = 1, d_{1,\mathrm{des}} = -4\,\mathrm{deg}, a_{2,\mathrm{des}} = 0.95, c_{2,\mathrm{des}} = 1$, and $d_{2,\mathrm{des}} = -4\,\mathrm{deg}$. The slow oscillations in the interaction torques stem from oscillations of parameters c. Z_3 and Z_4 factors demonstrate that the minimization of the functional containing the trajectory accelerations was rather good ($Z_{3,4} < 0.5$) (Fig. 5, panel C). Z_1 and Z_2, however, show that the adaptation of the parameter d_1 and the parameters a_1 and c_1 also led to good minimization of the torque functional (6) in the case of hip trajectory ($Z_1 < 0.6$), but that the resulting knee torque minimization was not so good ($Z_2 > 1$) (Fig. 5, panel B). This means that in this example, the parameter d_2 was not adapted as desired. Fig. 6, in turn, shows the achieved adaptation in terms of the hip (panel A) and knee (panel B) joint angle trajectories (impedance-based approach results). It can be observed that the adapted hip and knee trajectories are closer to the desired than the initial trajectories, but do not achieve a perfect match. It is unlikely to achieve a perfect match due to the used optimization method that does not guarantee global optimality (steepest-descent minimization, finite number of iterations with decreasing step sizes), due to parameterization of the gait trajectories, and due to oversimplified interaction and Lokomat models.

B. Experimental Results

1) Healthy Subjects: In the experiments a), most subjects were able to tell if the adaptation was enabled ($29/40 = 72.5\%$) or disabled ($26/38 = 68.4\%$). The fact that in some cases the subjects incorrectly classified the adaptation mode shows that the evaluation of the algorithms based on subject's opinion is not completely objective. Therefore, it was important to combine it with the analysis of the actual parameter changes. The enabled adaptation led to reduction in the interaction torques, opposed to interaction torques that remained high in the case of disabled adaptation. The main algorithm performance comparison was done between the direct dynamics and the impedance-control-based algorithms. The evaluation of parameter adaptation revealed that the impedance-control-based algorithm performed best and most consistently.

The healthy subjects could well influence the gait pattern with their own effort. This is demonstrated in Fig. 7 for the direct dynamics (panel A) and the impedance control (panel B) algorithms. This figure shows the adaptation of the hip (left) and knee (right) walking-trajectory parameters. Solid bars indicate the time period where the subject tried to decrease hip and increase knee flexion, and the dashed bars indicate

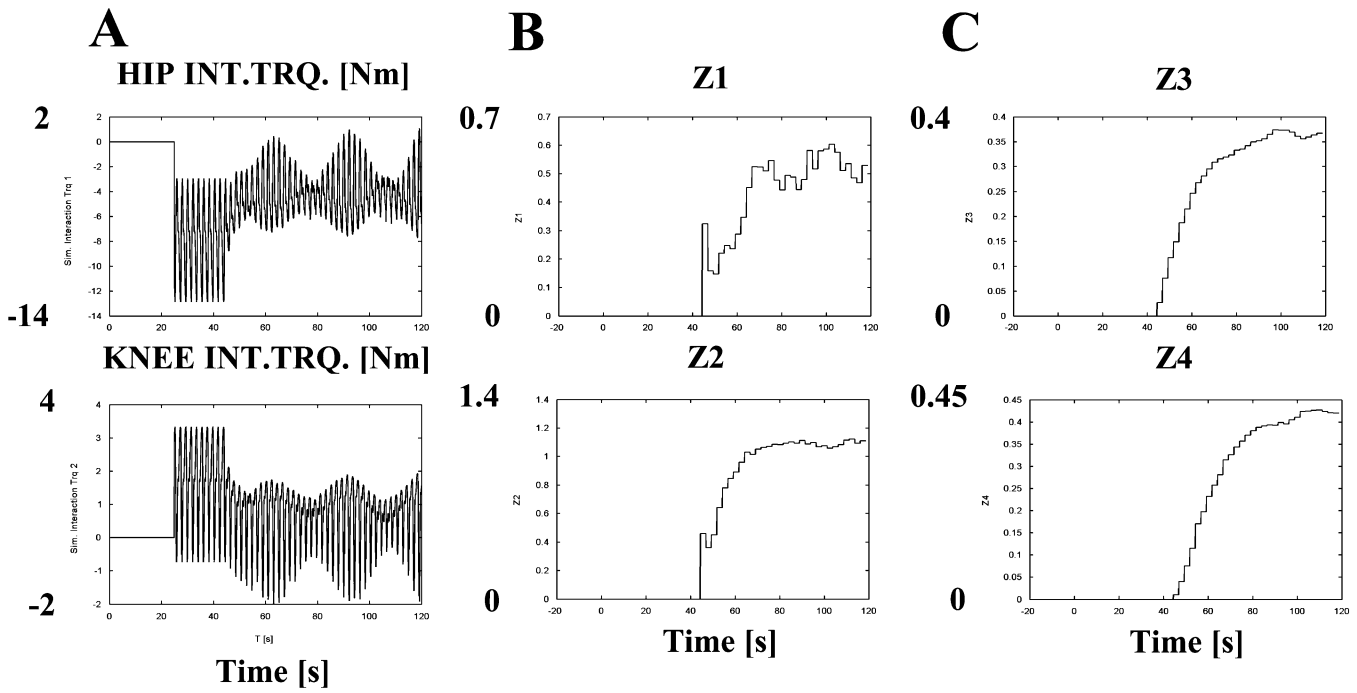

Fig. 5. Example showing the course of the hip and knee interaction torques (panel A), and the Z factors (panels B and C) during a computer simulation of the gait-pattern adaptation with a direct-dynamics-based algorithm.

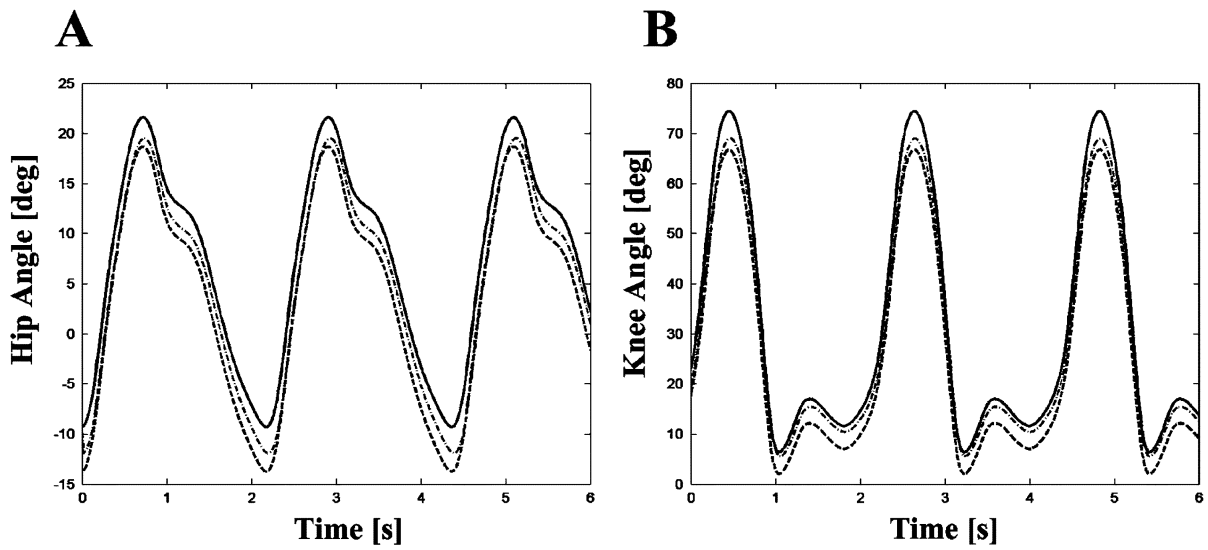

Fig. 6. Depicted is the adaptation in the hip (panel A) and knee (panel B) joint angle trajectories obtained with the impedance-control-based algorithm in computer simulations. The initial trajectories are plotted in solid lines, the desired trajectories in dashed, and the adapted trajectories in solid-dashed lines.

the period where the subject tried to do the opposite. Smaller a and d values mean decreased flexion. The adaptation of the knee parameters was better when the impedance-control-based algorithm was used, whereas the adaptation of the hip parameters was similar in both algorithms.

The experiments from b) and c) in all cases led to a significantly changed gait pattern that was, in most cases, close to the desired one. The adaptation of the unphysiological initial gait pattern in c) always resulted in a more physiological gait pattern. An example of an experiment from c) is shown in Fig. 8 (impedance-control-based algorithm). Panel A shows the parameter adaptation (subject tried to change the initial walking pattern after stride number 60 to a preferred one), and panel B the corresponding change of the initial (solid lines) to the adapted (dash-dotted lines) hip and knee trajectories (the parameters were averaged from strides 60 to 96 for the calculation of the adapted trajectory). The nominal trajectories are also plotted (dashed lines). One can see that for positive hip angles, the adapted trajectory got closer to the nominal trajectory, but for negative hip angles, it deviated more from the nominal than the initial trajectory. Still, the root mean square difference between the adapted and nominal versus nominal and initial trajectories has decreased (from 2.38° to 1.89°). The adaptation of the knee trajectory was smaller. The adapted trajectory approached the nominal one for small knee angles, and the difference between the adapted and nominal trajectory decreased from initial 9.83° to 8.35°. The preferred trajectory, however, most likely differs from the nominal one, and therefore, it is more important to observe that the adapted trajectory resulted in a more physiological walking than the initial one.

2) SCI Subjects: The SCI subjects were able to influence the gait pattern with their remaining voluntary activity [experiments b)]. The extent of gait-pattern adaptation depended, of course, on the force that

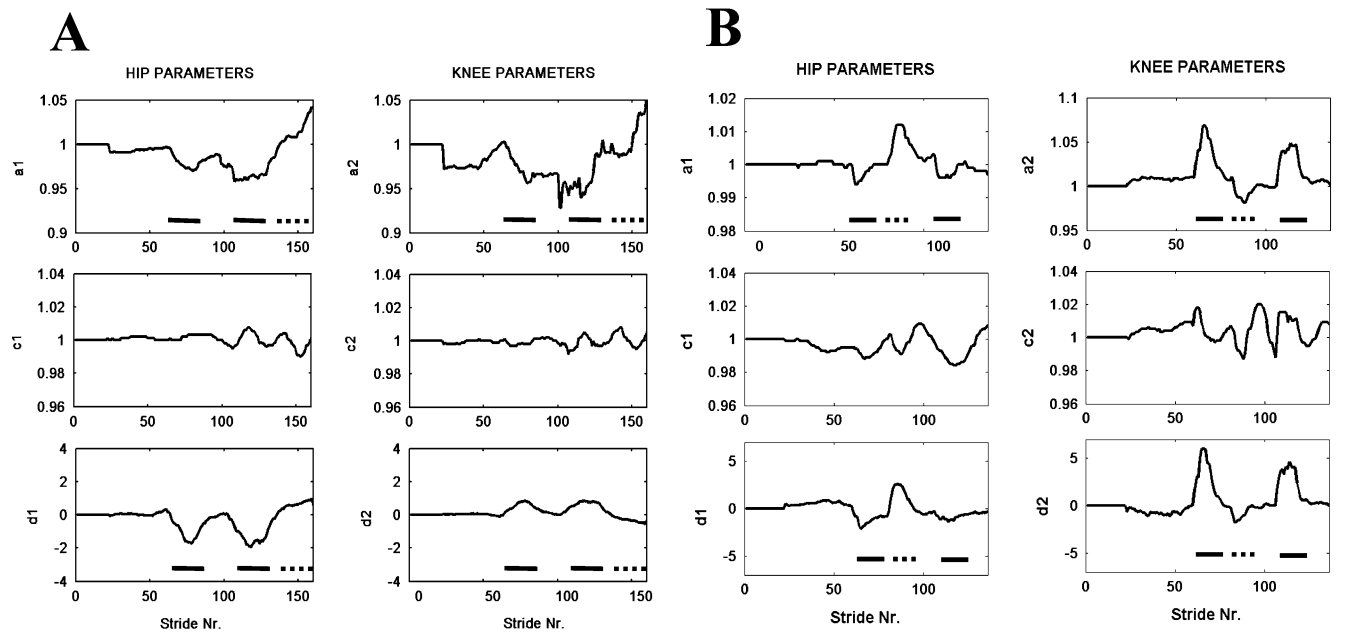

Fig. 7. Trajectory parameter adaptation obtained in an actual experiment with a healthy subject. Panel A shows the results for the direct dynamics, and panel B for the impedance-control-based algorithm.

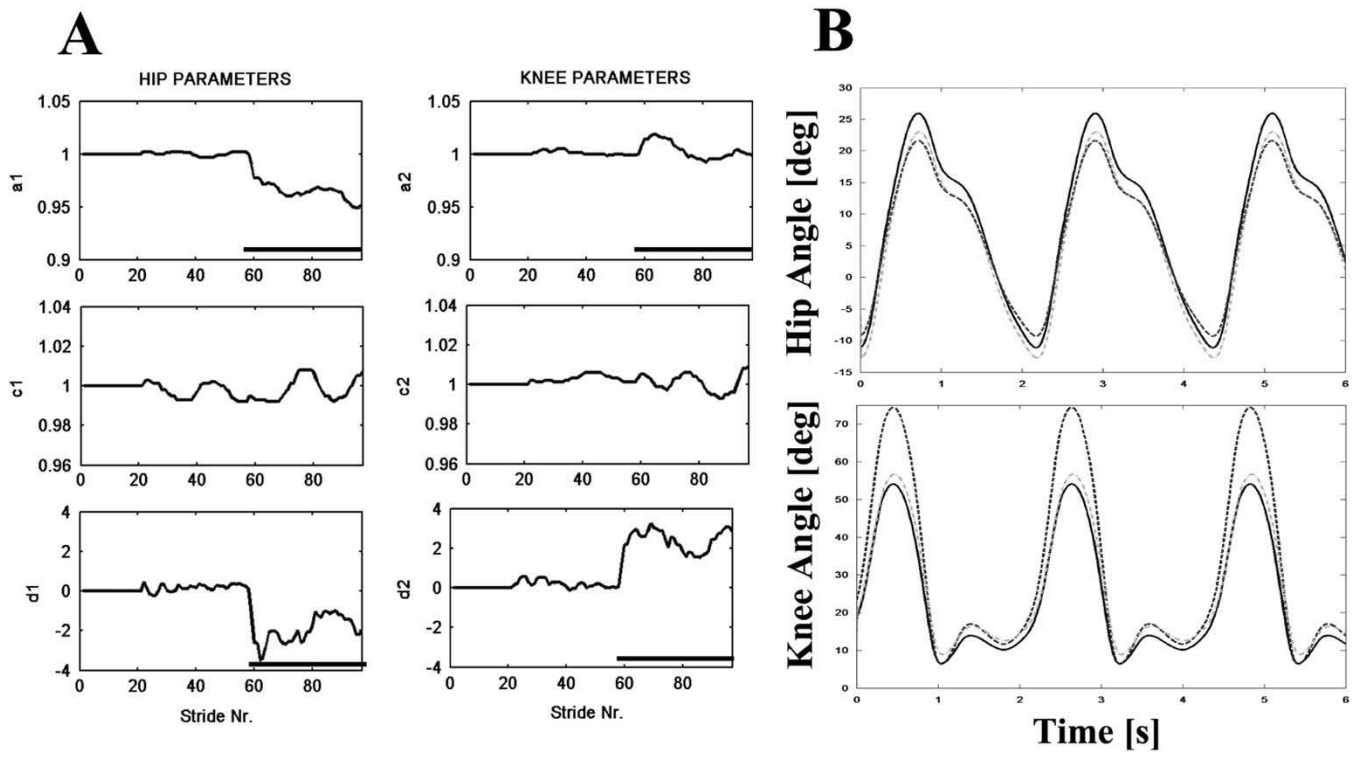

Fig. 8. Gait-pattern adaptation obtained in an actual experiment with a healthy subject that started walking with increased hip and decreased knee range of motion (unphysiological initial gait pattern). Panel A shows the adaptation in trajectory parameters, and panel B the adaptation in terms of joint angles. The initial trajectories are plotted in solid lines, the nominal trajectories in dashed, and the adapted trajectories in solid-dashed lines.

they were able to produce. Usually, they could achieve large adaptation for periods up to 5–10 min. Like the healthy subjects, the patients were able to adapt the gait pattern from experiments b) to be like the desired one. An example of gait-pattern adaptation for a SCI subject is shown in Fig. 9. The thin bars indicate the time where the patient tried to walk faster, the thick bars the time where he tried to walk with larger steps, and the dashed bars the time where he tried to walk with shorter steps. The first period resulted in increased hip flexion (increased a_1 and d_1), slightly reduced knee flexion (decreased a_2), and slight increase in the speed (reduced c_2). The second period resulted in increased, and the third one in reduced hip and knee flexion. Such an adaptation outcome is in line with the desired changes.

Most of the patients, however, had problems with following and adapting the unphysiological initial gait pattern [experiments c)]. Their feet (or one foot) hit the treadmill during the swing phase so that they were tripping over. We had to unload them almost completely to pre-

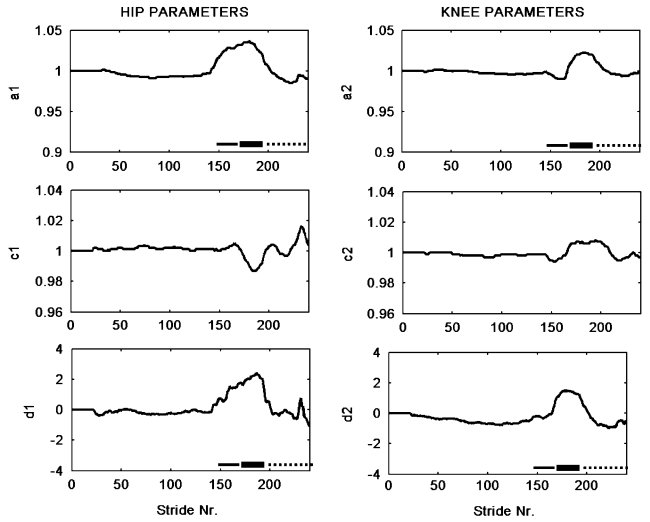

Fig. 9. Example of gait-pattern adaptation for a SCI subject. The thin bars indicate the time where the patient tried to walk faster, the thick bars the time where he tried to walk with larger steps, and the dashed bars the time where he tried to walk with shorter steps.

vent this tripping, which was not always possible to completely avoid. The gait pattern, in many cases, remained unphysiological or sometimes even adapted to an even more unphysiological one.

At the end, we would like to mention that no obvious correlation between the level of the injury and the training performance could be observed.

IV. Discussion and Conclusions

This paper has dealt with the problem of automatic gait-pattern adaptation for a robotic device used in rehabilitation of locomotion. Three different approaches to the solution of the problem were presented that were based on physical laws or on a special closed-loop control algorithm. Because the algorithms are based on basic physical and control theoretical considerations, they could also be used in other human–robot interaction problems, and are not limited to the application treated in this paper.

The performance of the algorithms was tested in computer simulations and in actual experiments with healthy and SCI subjects. A satisfactory adaptation was achieved in all cases, with better adaptation of the hip than the knee trajectories. Computer simulations and actual experiments have shown that the direct-dynamics-based algorithm performed better than the inverse-dynamics-based algorithm. Best performance in experiments was achieved by the impedance-control-based approach. These results were also confirmed by a clinical study (see below) (Jezernik *et al.* [10]).

All three algorithms had problems when tested with SCI subjects that started walking with an unphysiological initial gait pattern. The algorithms were not always able to adapt this gait pattern to a more physiological one. This does not present a real problem, as it does not make sense to perform actual rehabilitation training with an unphysiological gait pattern.

Another important point in connection with the impedance control is the possibility of introducing impedance-magnitude adaptation into the control scheme. This would allow yet another gait-pattern adaptation principle, where the impedance would be set high in case of little patient effort to change the gait pattern, and where the impedance would be modulated (reduced) as an increased patient effort is detected. This would enforce small deviations from the reference motion when the patient would not want to change this motion, and allow for larger deviations from the reference motion in case that the patient would want to walk in another way. The exploration of this algorithm is currently a topic of our research, and an initial feasibility study has been completed (Gareiss [4], Jezernik [9]).

Important is also the possibility to modify the extent of adaptation. This is possible by modifying the gradient search step sizes, or, more conveniently, by modifying the value of the adaptation scaling w. The extent of the allowed adaptation can be set by a physiotherapist according to the condition and progress of the patient.

A more precise, statistical evaluation of the gait-pattern adaptation experiments with patients is under way (clinical study involving six patients), and will be published elsewhere (Jezernik *et al.* [10]). The impedance-control-based gait-pattern adaptation algorithm is planned to be commercialized to augment the treatment modalities of the Lokomat.

Acknowledgment

The authors would like to thank R. Schreier for his technical assistance.

References

[1] H. Barbeau, M. Ladouceur, K. E. Norman, and A. Pepin, "Walking after spinal cord injury: Evaluation, treatment, and functional recovery," *Arch. Phys. Med. Rehabil.*, vol. 80, pp. 225–235, 1999.

[2] G. Colombo, M. Joerg, R. Schreier, and V. Dietz, "Treadmill training of paraplegic patients with a robotic orthosis," *J. Rehabil. Res. Dev.*, vol. 37, pp. 693–700, 2000.

[3] V. Dietz, G. Colombo, L. Jensen, and L. Baumgartner, "Locomotor capacity of spinal cord in paraplegic patients," *Ann. Neurology*, vol. 37, pp. 574–582, 1995.

[4] V. Gareiss, "Moderne Regelungskonzepte für die Gangorthese Lokomat," Diploma thesis, Automat. Control Lab., ETH, Zürich, Switzerland, 2002. (in German).

[5] S. Hesse, C. Bertelt, M. T. Jahnke, A. Schaffrin, P. Baake, M. Malezic, and K. H. Mauritz, "Treadmill training with partial body weight support compared with physiotherapy in nonambulatory hemiparetic patients," *Stroke*, vol. 26, pp. 976–981, 1995.

[6] N. Hogan, "Impedance control: An approach to manipulation. Parts I, II, and III," in *J. Dynam. Syst., Meas., Contr.*, vol. 107, 1985, pp. 1–24.

[7] S. Jezernik, G. Colombo, and M. Morari, "Joint-angle trajectory adaptation for the robotic orthosis Lokomat," in *Proc. Workshop on European Scientific and Industrial Collaboration*, Enschede, The Netherlands, 2001, pp. 451–456.

[8] S. Jezernik and M. Morari, "Controlling the human-robot interaction for robotic rehabilitation of locomotion," in *Proc. 7th Int. Workshop Advanced Motion Control*, Maribor, Slovenia, July 2002, pp. 133–135.

[9] S. Jezernik, K. Jezernik, and M. Morari, "Impedance-control-based gait-pattern adaptation for robotic rehabilitation device," in *Proc. 2nd IFAC Conf. Mechatronic Systems*, Berkeley, CA, Dec. 2002, pp. 417–421.

[10] S. Jezernik, R. Schärer, G. Colombo, and M. Morari, "Adaptive robotic rehabilitation of locomotion: A clinical study in spinally injured individuals," *Spinal Cord*, vol. 41, no. 12, pp. 657–666, Dec. 2003.

[11] B. Siciliano and L. Villani, *Robot Force Control*. Norwell, MA: Kluwer, 1999.

[12] D. Šurdilović and Z. Čojbašić, "Robust robot compliant motion control using intelligent adaptive impedance approach," in *Proc. IEEE Int. Conf. Robotics and Automation*, Detroit, MI, 1999, pp. 2128–2133.

[13] A. Wernig, S. Müller, A. Nanassy, and E. Cagol, "Laufband therapy based on "rules of spinal locomotion" is effective in spinal cord injured persons," *Eur. J. Neurosci.*, vol. 7, pp. 823–829, 1995.